Iraqi Journal of Physics, 2024 *Vol. 22, No. 4, PP. 42-52*
https://doi.org/10.30723/ijp.v22i4.1290
P-ISSN: 2070-4003
E-ISSN: 2664-5548

Sensitivity of Newly Prepared Nanomaterials to NO_2 Gas and its Importance on Environmental and Industrial Safety

Sara Thualfuqar Jamil[1a*] and Basim Ibrahim Al-Abdaly[1,2b]
[1]*Department of Chemistry, College of Science, University of Baghdad, Baghdad, Iraq*
[2]*Department of Biology, College of Science, Uruk University*
[a*]Corresponding author: sara.jameel2305@sc.edu.uobaghdad.iq

Abstract

Polyaniline (PANI) and manganese dioxide (MnO_2) doped with nickel oxide (NiO) nanocomposite have emerged as promising materials for gas sensing applications due to their high conductivity and surface area. This study improves the synthesized PANI/MnO_2:NiO nanocomposites' sensitivity towards NO_2 gas. Atomic force microscopy (AFM), Fourier transfer infrared (FTIR), scanning electron microscopy (SEM), energy-dispersive X-ray analysis (EDS), and X-ray diffraction (XRD) were used to analyze the produced nanocomposites. More precise methods were investigated to identify problems associated with oxidation, corrosion and sensor activity, such as increasing the amount of added nickel oxide, changing the structure of nanocomposites, and regulating the working temperature and humidity. Based on the results of this study, it is critical to comprehend how sensitive nanomaterials are to NO_2 gas because exposure to this pollutant can negatively impact the environment and human health. Strategies to reduce its effects and improve industrial and environmental safety can be devised based on how nanomaterials react to nitrogen dioxide gas. We also examine antioxidants and PANI/MnO_2:NiO nanocomposites for their anti-corrosion properties to guarantee long-term stability with the sensor's conductivity. Strong antioxidant and corrosion-resistant substances should be added to the sensor to extend its lifespan and maintain its performance under challenging operating conditions. Integrating these sensitive nanomaterials into gas-sensing devices can significantly improve environmental monitoring and industrial safety protocols, ultimately contributing to better air quality management and public health protection.

Article Info.

Keywords:
Polyaniline, Gas Sensor, Nanocomposites, Response Time, Recovery Time.

Article history:
Received: May,04, 2024
Revised: Aug. 23, 2024
Accepted: Sep. 08, 2024
Published:Dec. 01,2024

1. Introduction

Gas analyzers and sensors are essential for regulating technological processes and determining the industrial production of hazardous and lethal compounds. The need for these devices is increasing due to several factors, including the obvious improvement in industry. Many of these technological processes can be improved or failed, depending on the reaction speed and reliability of automatic analytical devices based on gas sensors, whether used independently or as part of control systems [1]. The emergence of nanotechnology has facilitated significant advancements in the field of sensing due to the distinctive characteristics of nanomaterials, including high surface area to volume, surface active site, and extremely high surface reactivity [2]. Particular interest in their creation has been sparked by the qualities of nanomaterials, which include strong chemical and thermal durability, high electrical conductivity, distinct catalytic activity, and huge surface area [3]. Semiconductor nanostructures exhibit size-dependent characteristics that differ from those of large semiconductors [4]. The metal oxide (MO) chemo-resistive gas sensor is known for its excellent stability, affordable price, and simple connectivity with electronics. Doping metal oxides (MOs) with additional catalytic metals greatly increases the MOs gas sensor's sensitivity and specificity. When gases, such as O_2, CO_2, and NO_2, interact with the metal oxide surface, they take

electrons from it and act as electron donors; hence, these gases can be categorized as reducing gases [5]. A major category of inorganic nanomaterials, transitional metal oxide nanoparticles have been thoroughly studied because of their intriguing catalytic, magnetic, and electronic properties concerning their bulk counterparts, as well as their numerous potential uses when compared to bulk materials [6]. When used as sensing materials, nanoparticles, such as TiO, ZnO, MnO_2, and CoO, work well in detecting NO_2. However, the high operating temperature of these sensorsis a clear drawback that leads to excessive energy use and integration challenges [7]. Polymeric materials are extremely desirable and superior to other industrial materials in many applications. Easy chemical modification, low cost, compact size, better insulation and ease of production are some of these attributes [8]. Gas sensors that utilize organic conducting polymers, such as polyaniline (PANI), polypyrrole (PPy), polythiophene (PTh), etc., and possess the requisite feature set and conductivity, are continuously advancing in their capabilities [9]. Many researchers have utilized NiO as a sensing material for formaldehyde detection. Additionally, it has been employed as a dopant in polyaniline (PANI) for the same purpose. While most metal oxide sensors typically require high temperatures exceeding 100°C for operation, NiO is capable of detecting ethanol at room temperature. This characteristic enhances NiO's potential for sensing analytes across a wide temperature range, both high and low [10].

The aim of this research work is to explore the synthesis of (PANI/MnO_2:NiO) polymer matrix composites that combine with PANI nanoparticles to improve the optical, chemical and physical properties of the materials. The study aims to optimize the synthesis settings and investigate the morphological, structural and functional properties of the composites. Also, to provide data that can assist industries in meeting regulatory standards for NO_2 emissions, thereby promoting sustainable practices, to contribute to the development of advanced materials that can be used for real-time monitoring of air pollutants, paving the way for innovative solutions in environmental protection and industrial safety. These composites may find application in the future in nitrogen dioxide gas sensing by improving environmental monitoring systems and promoting the development of safer industrial practices [11].

2. Experiential Work

2.1. Materials and Method

Aniline C_6H_7N (ANI) of (99.5%) purity were supplied from Pub chem. All the other chemicals, manganese (II) sulfate ($MnSO_4$), potassium permanganate ($KMnO_4$), nickel (II) acetate ($Ni(CH_3CO_2)_2$), hydrochloric acid (HCL), were purchased from Sigma Aldrich. The nanocomposite was prepared using a refined deionized aqueous framework. The following components were used without further filtration: ethanol (C_2H_6O), sulfur, and ammonium sulfate $(NH_4)_2S_2O_8$ (APS). This work prepared metal oxides and nanocomposites using sol-gel and hydrothermal processes, Atomic forc microscopy (AFM), Fourier transfer infrared (FTIR), scanning electron microscopy (SEM), energy-dispersive X-ray analysis (EDS), and X-ray differeaction (XRD) techniques were used to characterize them.

2.2. Synthesis of MnO_2 by Sol-Gel Method

A mixture of $MnSO_4$ 4.22g (1.0M) and $KMnO_4$ 1.97g (0.5M) solution was dissolved in 50ml of deionized water with stirring for 4 h at 70°C. After removing contaminants with ethanol and distilled water multiple times, the precipitates were vacuum-dried for five hours at 110°C. The dehydrated powder was placed inside a muffle and heated at 300°C for an extra three hours. 2.0M H_2SO_4 was used to acidify

these powders for two hours at 90°C. The result was then vacuum-dried after being cleaned with distilled water [12].

2.3. Synthesis of NiO by Hydrothermal method

3.117g $Ni(CH_3CO_2)_2$ salt of 0.5 M was added to 25 ml of deionized water. Once they had dissolved, 0.08 g, 0.5 M of the combination was put in a Teflon linear autoclave cell after melting in ten milliliters of deionized water. It was heated for 24 hours at 150°C with a heating rate of 2°C per minute. Following the cooling of the cell, the mixture was sorted using centrifugation at 4000 rpm for 15 minutes. The separated sample was then dried in an oven at 75°C [13].

2.4. Synthesis of Nanocomposite of PANI/[MnO_2/NiO] by in Situ Polymerization Method Using Sol-Gel Method

PANI/MnO_2/NiO nanocomposite samples were created using ammonium persulfate acting as an oxidizing agent during the in situ oxidative polymerization of aniline in the presence of MnO_2/NiO nanoparticles in an acidic mixture. The PANI/MnO_2/NiO nanocomposite was made by aggressively stirring 70 ml of 2M HCl and 4.5 ml of distilled aniline for 30 minutes at room temperature in a magnetic stirrer. 4.5g of APS was then dissolved using 20 ml of deionized water that contained one weight per cent MnO_2/NiO and 0.05g of sodium dodecyl sulfate (SDS) nanoparticles. This solution was added dropwise to the first solution. An excellent degree of polymerization was indicated by the solution's turning green color with the addition of APS containing MnO_2/NiO. Stirring was continued for a further two hours. The precipitate was filtered and then dried. PANI/MnO_2/NiO (10 wt%) was obtained from the final result of the nanocomposite [14].

3. Results and Discussion

AFM, FTIR, and SEM-EDS were employed to study the properties of these nanocomposites, such as size, morphology, and dispersion.

3.1. Atomic Force Microscopy (AFM)

Surface morphology and roughness of PANI\ [NiO: MnO_2] nanocomposite prepared by sol-gel method were studied from the 3D AFM images shown in Fig. 1. The NiO coating is significantly smaller than the PANI coating. The morphology has changed due to the MnO_2 doping in the PANI coating. According to the homogeneous coating, doping of MnO_2:NiO with PANI has enhanced the microstructure of PANI/MnO_2:NiO regarding the ability to conduct electricity of the interaction. The results confirm that the average standard deviation (Rq) was 7.31 nm and the typical roughness (Ra) was 4.55 nm. The average measurement conveyed by the analysis of the nanocomposite indicated that the average size of the molecules was 88.76 nm. AFM images showed how the Sol-gel method had organized the nanocomposite [15].

3.2. Scanning Electron Microscopy and Energy Dispersive X-ray (SEM/EDS)

Fig. 2 displays the morphology of the as-prepared materials using the field emission on SEM. The PANI/MnO_2:NiO nanocomposite was noted to be rough, as seen by the SEM images. As a result of electrodeposition, MnO_2 nanoparticles were widely dispersed across the surface. Additionally, the homogeneous thickness suggested that PANI and MnO_2:NiO are co-deposited. The surface had risen due to the presence of MnO_2:NiO nanoparticles, which is advantageous for the transport of electrolytes and accessibility to active sites. Fig. 3 displays the elemental analysis using EDS of the

PANI/MnO2:NiO compound, confirming the existence of MnO_2 and NiO in the composite [16].

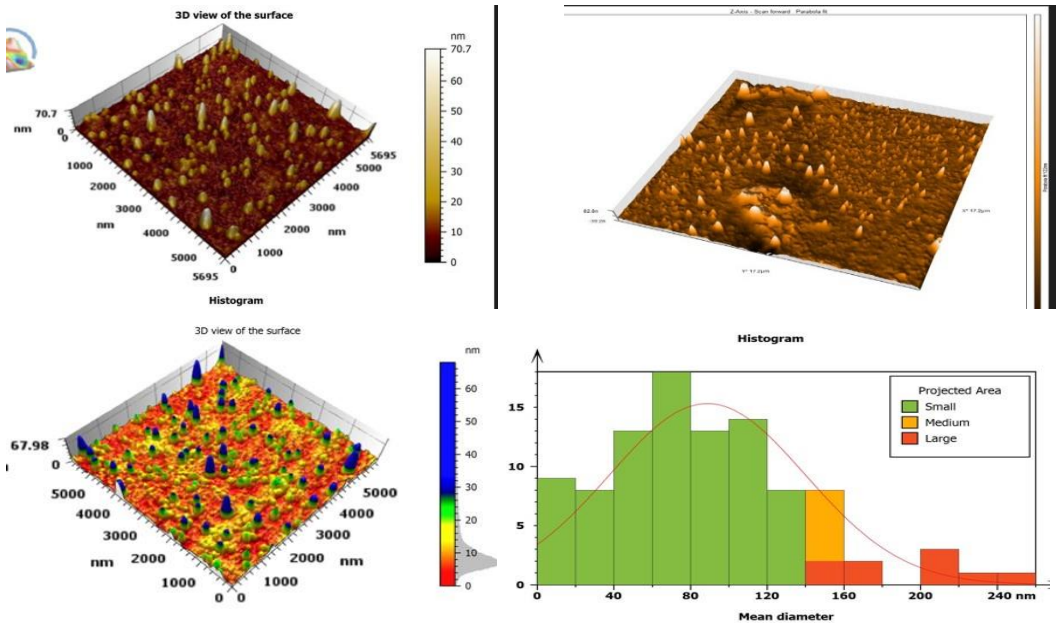

Figure 1: 3D AFM images the nanostructure and particle size distribution of the prepared MnO_2:NiO and PANI nanocomposites.

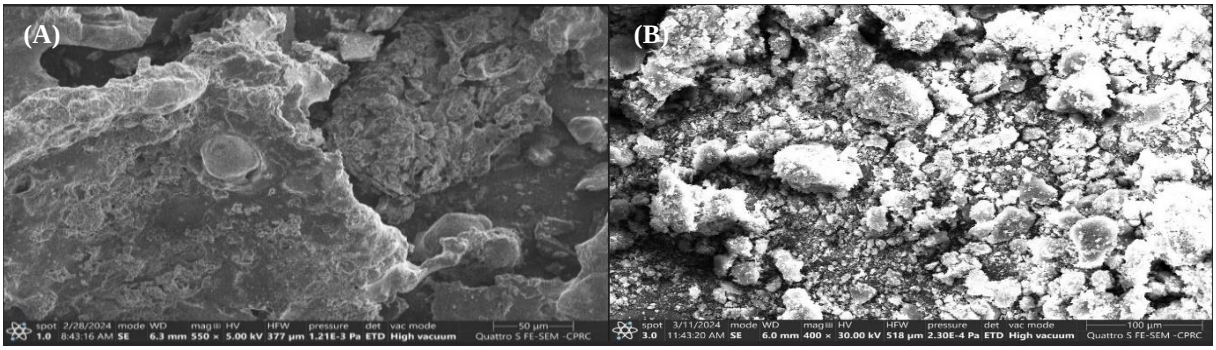

Figure 2: The SEM Images (A, B) of PANI/MnO_2:NiO nanocomposite with different magnifications 50Kx, and 100 Kx, respectively.

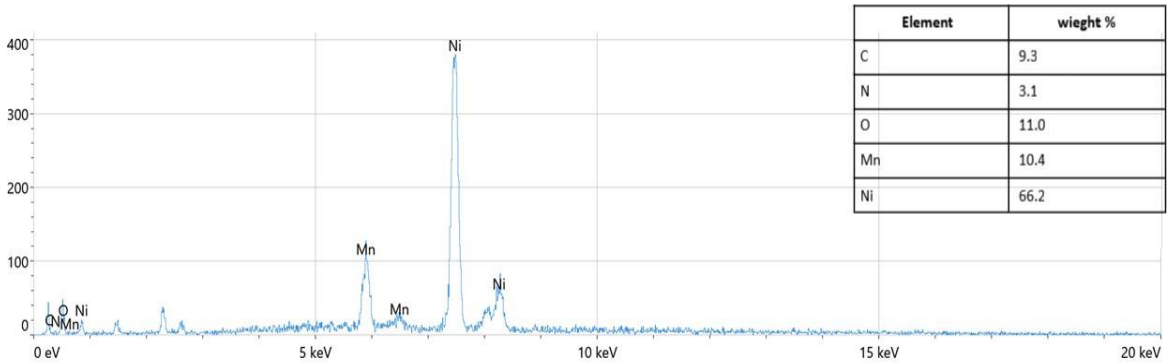

Element	wieght %
C	9.3
N	3.1
O	11.0
Mn	10.4
Ni	66.2

Figure 3: EDS of PANI/MnO_2:NiO nanocomposite.

3.3. Fourier Transform Infrared Spectroscopy Analysis (FT-IR)

FTIR spectra of PANI/MnO_2: NiO nanocomposite, MnO_2, and NiO were collected to gather more detailed information. As depicted in Fig. 4, PhN, benzenoid structure, and quinoid structure are responsible for the peaks at 1308, 1506, and 1623 cm^{-1}, respectively. The bands indicated the C-C stretching of quinoid and benzenoid rings at 1623 and 1506 cm^{-1}, respectively. The aromatic amine's C-N stretching band was represented by the bands in the 1390–1400 cm^{-1} range. The N-H stretching is as specified by the band at 3320 cm^{-1}. Furthermore, the peak at 560 cm1 is caused by the Mn-O vibrations. Both elements in the composite were confirmed by the FTIR spectrum of the MnO_2 respective distinctive bands [17]. FTIR spectra of NiO showed the stretching mode of Ni-O, which was attributed to the peak centered at 423 cm^{-1}, providing unambiguous evidence for the creation of NiO nanoparticles [18].

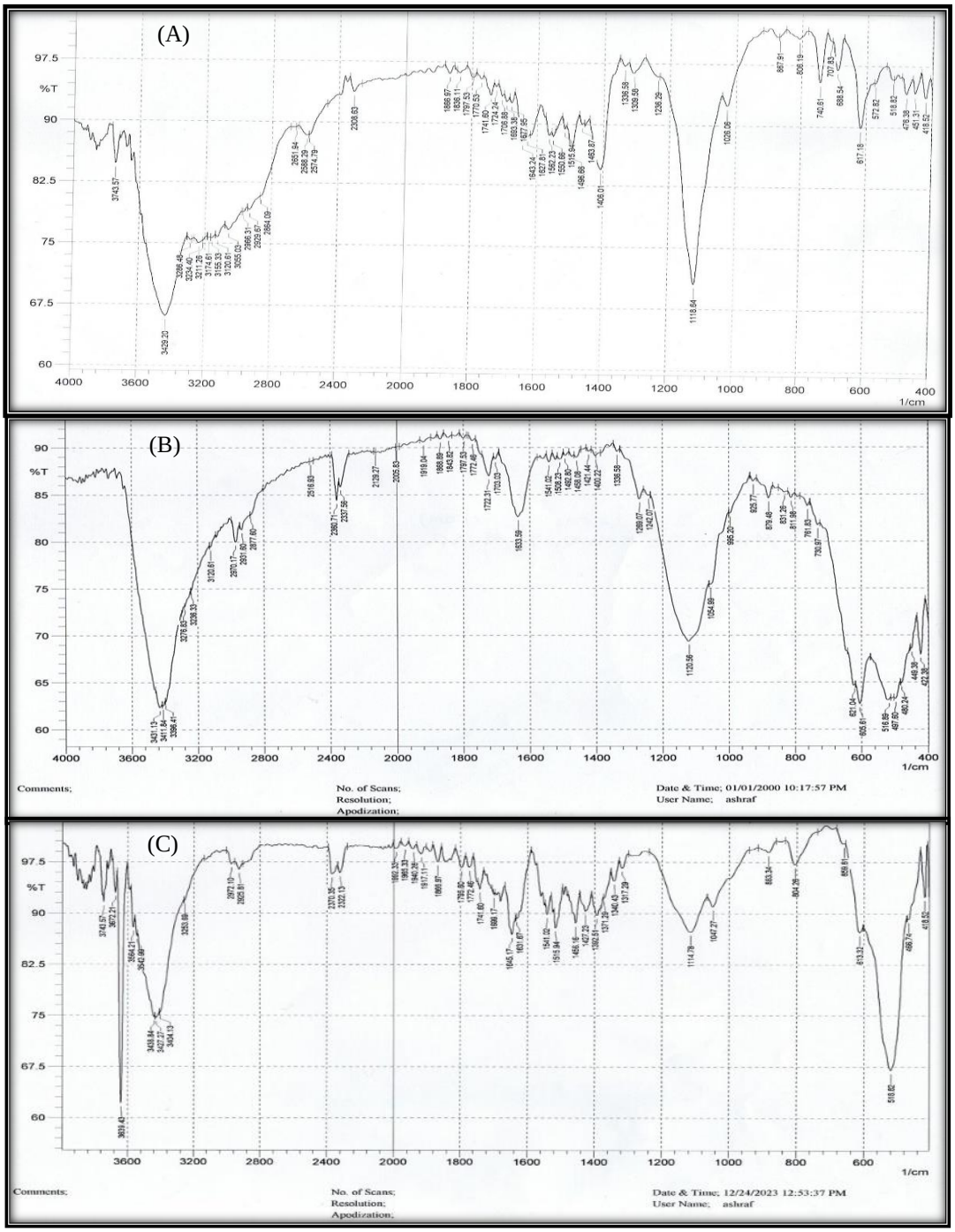

Figure 4: FT-IR spectra of (A) PANI/MnO_2: NiO nanocomposite (B) MnO_2 (C) NiO.

3. 4. X-ray Diffraction (XRD) Studies

Fig. 5 shows the XRD patterns of PANI/MnO_2:NiO nanocomposite. The XRD pattern of the pure MnO_2 suggested that the material crystallizes with acceptable crystallinity. The position of peaks for MnO_2 corresponds to the same last Miller indices 111, 212, 222, 141, and 133, along with angles of rhombohedral structures at $2\theta^{o}$ = 37˚, 43˚, 63˚, 75˚, and 79˚ identified by applying standard data (JCPDS no. 01-084-0542). The results obtained are reasonably consistent with the one given by Obodo et al. [19]. The average crystallite size of the pure manganese dioxide nanoparticles was reported to be 24.2 nm. The NiO-NP XRD pattern showed peaks at 2θ =°15.18,°24.05, °29.12,°35.15,°44.30 and °47.25 corresponding to the same Miller indices (111, 200, 212, 222, 141 and 400), respectively. This matched rhombohedral crystal structure and the reference cards (JCPDS card No. 00-022-1189). Using the X'Pert high score program, the sample's average crystal size (D) was determined to be 27.5 nm [20]. The average crystalline size of PANI/MnO_2:NiO nanoparticles was 30.5 nm. The determination refers to the prominent peaks of the pattern diffractogram by applying the Debye Scherrer's equation

$$D = \frac{K\lambda}{\beta\cos\theta} \qquad (1)$$

where D is the crystallite size, K is the Scherrer constant (0.9), λ is the wavelength of the X-ray used of 0.15406nm, β is the Full Width at Half Maximum (FWHM, radians), and θ is the peak position (radians) [21].

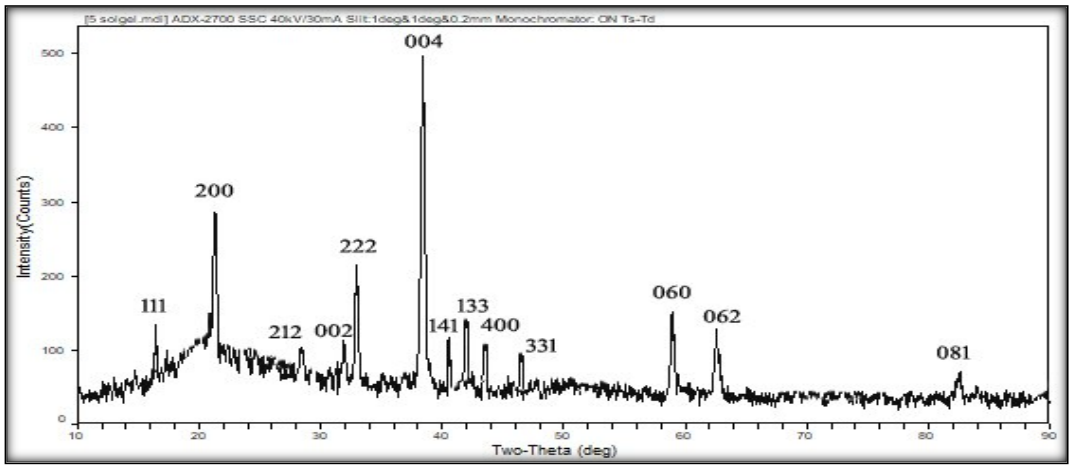

Figure 5: XRD pattern of PANI/MnO_2:NiO nanocomposite.

4. Corrosion Protectiveness Studies

Corrosion solutions are crucial for developing effective gas sensors, as corrosion can significantly impact stability, sensitivity, and selectivity of the sensing materials. Researchers often aim to create protective coatings or choose corrosion-resistant materials to enhance the performance of gas sensors in various environments. Corrosion products can introduce new active sites on the sensor surface, potentially affecting its selectivity toward specific gases in materials like PANI, which is used in some gas sensors, corrosion can change the conductivity of the polymer. Protonation and deprotonation processes in response to gas exposure are crucial for sensing mechanisms; any corrosion-related changes can interfere with these processes. Gas sensors often rely on surface reactions between the target gas and the sensing material. Corrosion can alter the surface properties, such as roughness and chemical reactivity, affecting how gases interact with the sensor material.

Corrosion parameters are evaluated according to the data shown in Table 1 and Fig. 6. Corrosion current rate (i_{corr}), and the possibility of corrosion (E_{corr}) solution of 0.1M HCl as a blank used for the corrosion testing, were acquired by extrapolating the anode (b_a) and cathode (b_c) Tafel slopes are also calculated. Table 1 shows the results of corrosion potential the results of corrosion potential E_{corr} (mV), corrosion current density i_{corr} (A/cm^2), cathodic and anodic Tafel slopes (mV/Dec), and protection efficiency PE(%) in Eq.(2) [22, 23]

$$\%IE = \frac{(i_{corr})_o - (i_{corr})_i}{(i_{corr})_o} \times 100 \qquad (2)$$

where $(i_{corr})_i$ is the corrosion current density in the absence of inhibitors, and $(i_{corr})_o$ is the corrosion current density in the presence of inhibitors [23].

Table 1: The corrosion parameters for compound NiO:MnO_2/PANI substances and a blanks in HCl solutions.

Comp.	E_{corr}	I_{corr}	I corr./r	Resis.	Anodic βa	Cathodic βc	Corr. rate	IE%
Blank	-0.405	376.3	7.526E-4	62.73	0.139	0.089	3.694	-
PANI/ MnO_2: NiO	-0.744	44.74	8.948E-5	1388	0.256	0.325	0.439	85

The NiO:MnO_2/PANI sample under test was placed inside a corrosion cell, the surface area exposed to the solution was 16.55 cm^2. The full polarization measurement system configuration is displayed in Fig. 6 [24].

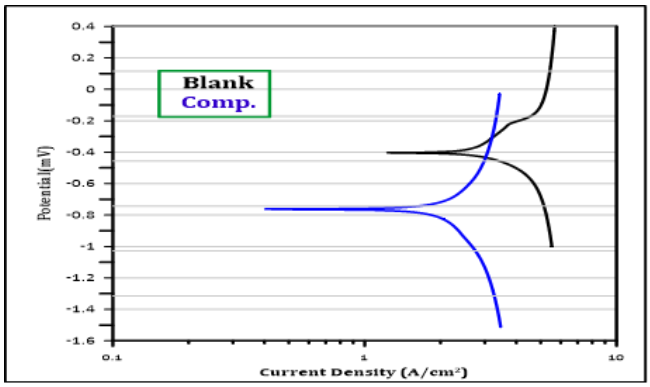

Figure 6: Polarization curves for corrosion of PANI/MnO_2:NiO.

5. Antioxidant Activity

The aim of the study is to evaluate the antioxidant activity of the NiO /PANI nanocomposite, with a focus on understanding how the incorporation of NiO and MnO_2 into PANI enhances its protective properties. By investigating this nanocomposite, the study seeks to determine its potential applications in mitigating oxidative stress, which can lead to various degradation processes in materials and biological systems. The synergistic effects of NiO and MnO_2 within the PANI matrix may provide a novel approach to developing effective antioxidant materials, thereby broadening the scope of PANI-based composites in fields such as biomedicine and materials science.

5.1. 1,1-Diphenyl-2-picrylhydrazyl (DPPH)

100 mm of methanol and 4 mg of 1,1-diphenyl-2-picrylhydrazyl (DPPH) were added in a test tube filled with aluminum foil. The solution was not exposed to light. A stock solution of 100 ppm concentration was prepared by dissolving 1 mg of NiO:MnO_2/PANI in 10 mL of methanol. Dilutions of (50, 25, 12.5, and 6.25 ppm) were produced from the stock solution.

5.2. Ascorbic Acid

The methanol extract's anti-oxidant effectiveness and consistent vitamin C were evaluated, as well as the stable free-radical DPPH's ability to scavenge radicals. The DPPH solution of 1 mL was added to one milliliter of the stock or diluted solutions of concentrations (100, 50, 25, 12.5, and 6.25 ppm) in a test tube. All solvents were tested for absorbance at 517 nm using a spectrophotometer, and they were then incubated for just one hour at 37 °C. Using Eq. (3), three measurements were taken. It can ascertain Diphenyl-2-picryl hydrazyl DPPH-scavenging potential.

$$I\% = [(Abs\ blank - Abs\ sample) / Abs\ blank] \times 100 \quad \textbf{(3)}$$

when compared to the DPPH-free, the recently created nanocomposite [25] showed antioxidant activity in Table 2 and Fig. 7.

Table 2: Antioxidant Activity according to Phongpaichit, 2007 [26].

Composite Concentration NO.	**100 µg/ml**	**50 µg/ml**	**25 µg/ml**	**12.5 µg/ml**	**6.25 µg/ml**	**Linear eq. y**	**R^2**	**IC_{50}**
PANI/MnO_2:NiO	73.91	66.96	64.35	56.52	55.22	-4.782x + 77.738	0.9597	5.8

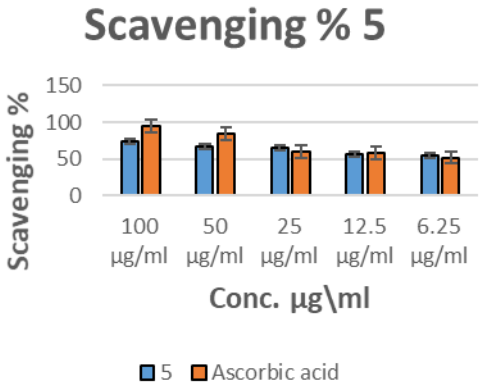

Figure 7: Antioxidant activity of PANI/MnO_2:NiO nanocomposite.

The antioxidant activity of the NiO/PANI nanocomposite, such as the percentage of DPPH scavenging and the efficacy at different concentrations, were deduced from the obtained results. An IC50 value of 5.8 µg/ml indicates that the composite is highly effective in scavenging DPPH radicals. This low concentration required for 50% inhibition suggests strong antioxidant properties, making it a promising candidate for applications where oxidative stress mitigation is critical, such as in potential applications in materials science or biomedicine.

6. Gas Sensing Data

NO_2 was used to analyze NiO:MnO_2/PANI for gas sensing at various operating temperatures, starting at ambient temperature and going up to 100, 150, and 200 K. The resistance of the sample(sensor) changes with time on exposure to the gas [27]. When the gas flow rate was between 80 and 100 parts per million, two distinct resistances were noticed, in the presence of the gas (R_{on}) and in the absence of the gas (R_{off}) [28]. The values of which are listed in Table 3 for different operating temperatures. It is very important to describe the relationship between the sensor's resistance (R) and sensitivity (S) to display the sensing data for the NO_2 gas [29]:

$$S\% = (R_{on}-R_{off}) / (R_{on}) \times 100\ \% \quad \textbf{(4)}$$

The other important factors are response and recovery times [30]. The amount of time it takes to get a 90% conductance maximum (in the case of reducing gas) or minimum (in the case of oxidizing gas) can be used to characterize the response time. Conversely, the amount of time needed to be within 10% of the initial start point is known as the amount of time required for recuperation [31] upon stopping the emission of an oxidizing or reducing gas [32] The following comparison was made between the data of (as sensors) at three distinct temperatures, as shown in Fig. 8 and Table 3.

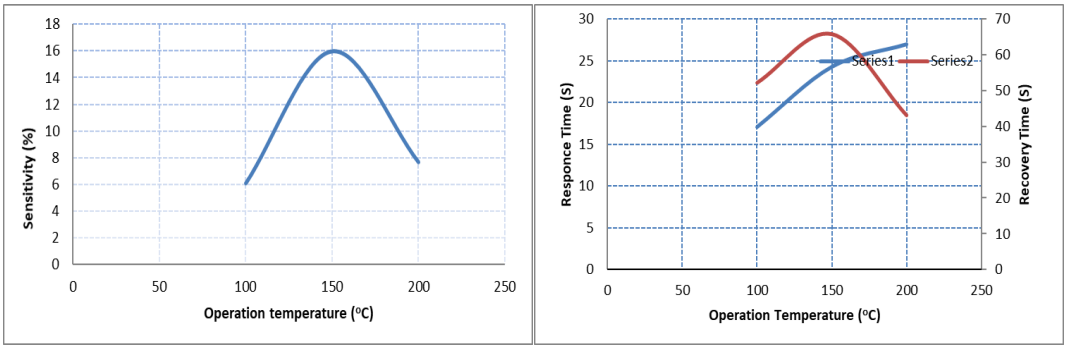

Figure 8. Sensing plots of PANI/MnO_2:NiO nanocomposite.

Table 3: The data of PANI/MnO_2:NiO nanocomposite for NO_2 sensing.

No.	Tem.(° C)	R_{on}(Ω)	R_{off}(Ω)	Sensitivity (S%)	Response time (sec.)	Recovery time (sec.)
1	100	37.02	34.89	6.104	17.1	52.2
2	150	19.15	16.51	15.990	24.3	65.7
3	200	3.753	3.485	7.690	27	43.2

The results indicate that increasing the temperature from 100 to 200°C significantly affects the sensing performance. R_{on} and R_{off} values decreased, suggesting enhanced conductivity and charge carrier mobility at higher temperatures. Sensitivity increased with temperature, peaking at 15.99% at 150°C and then declining to 7.69% at 200°C. This trend suggests an optimal sensing environment around 150°C, where the nanocomposite effectively responds to NO_2. Response times increased with temperature, indicating a slower detection process at higher temperatures, this trade-off suggests that higher temperatures improve sensitivity. Nanocomposite exhibits promising NO_2 sensing capabilities, with a balance between sensitivity and response/recovery times. This makes it suitable for applications in environmental monitoring where quick responses and sensitivity are essential.

The improvement process with the NiO material through its doping to PANI/MnO_2, in addition to the conditions that were controlled, such as temperature and the amount of reactants, also contributed to improving the properties of the prepared

nanocomposite and thus provided the possibility of using it as anti-corrosion and anti-oxidation materials, in addition to its use as a NO_2 gas sensor.

7. Conclusions

The development of PANI/MnO_2:NiO nanocomposites as NO_2 gas sensors has shown results in terms of improving sensitivity, sensor activity, anti-corrosion, and antioxidant properties. By optimizing the substrate (PANI/MnO_2) with the doping ratio of NiO, controlling the morphology of the nanocomposite, and fine-tuning operating conditions, we have successfully enhanced the sensor response to NO_2 gas while minimizing interference from other gases. Also, we have increased the sensor for a long time stability and dependability under demanding operating conditions by using it as an antioxidant and corrosion resistant antioxidant and corrosion-resistant chemicals. These improvements help the sensor last longer and continue to function well over time. PANI/MnO_2:NiO nanocomposites can function as efficient NO_2 gas sensors with improved anti-corrosion, antioxidant, and sensitivity, according to the study's general results. This study presents a dependable and effective method for identifying NO_2 gas in a variety of features, paving the way for the development of gas sensing systems for environmental monitoring and industrial safety applications.

Acknowledgment

The authors are grateful for permission from the Department of Chemistry, College of Science, University of Baghdad, to use their laboratories for scientific research.

Conflicts of Interest

The authors declare they have no competing interests.

References

1. H. J. Abdul-Ameer, M. F. Al-Hilli, and F. T. Ibrahim, Iraqi J. Sci. **64**, 630 (2023). DOI: 10.24996/ijs.2023.64.2.12.
2. Z. H. Mahmoud, O. D. Abdalstar, and N. Sabah, Earthline J. Chem. Sci. **4**, 199 (2020). DOI: 10.34198/ejcs.4220.199208
3. A. S. Elewi, S. a. W. Al-Shammaree, and A. K. M. A. Al Sammarraie, Sen. Bio-Sen. Res. **28**, 100340 (2020). DOI: 10.1016/j.sbsr.2020.100340.
4. A. J. Haider, A. A. Jabbar, and G. A. Ali, J. Phys. Conf. Ser. **1795**, 012015 (2021). DOI: 10.1088/1742-6596/1795/1/012015.
5. S. A. Hamdan, I. M. Ali, and I. M.Ibrahim, Iraqi J. Phys. **19**, 20 (2021). DOI: 10.30723/ijp.v19i50.629.
6. S. K. Abbas and A. N. Naje, Iraqi J. Phys. **18**, 62 (2020).
7. H. Zhang, J. Feng, T. Fei, S. Liu, and T. Zhang, Sen. Act. B Chem. **190**, 472 (2014). DOI: 10.1016/j.snb.2013.08.067.
8. A. Mohammed, M. Ghazi, and M. H. Suhail, Iraqi J. Phys. **15**, 122 (2017).
9. A. Kaushik, R. Kumar, S. K. Arya, M. Nair, B. D. Malhotra, and S. Bhansali, Chem. Rev. **115**, 4571 (2015). DOI: 10.1021/cr400659h.
10. N. Majdabadifarahani, M. Sc. Thesis, University of Waterloo, 2019.
11. A. A. Nemea and B. I. Al-Abdaly, Iraqi J. Sci. **65**, 1200 (2024). DOI: 10.24996/ijs.2024.65.3.3
12. A. P. Mahajan, S. B. Kondawar, and R. P. Mahore, Bion. Front., 173 (2017).
13. F. Fazlali, A. R. Mahjoub, and R. Abazari, Sol. Stat. Sci. **48**, 263 (2015). DOI: 10.1016/j.solidstatesciences.2015.08.022.
14. S. Vijayalakshmi, E. Kumar, M. Ganeshbabu, P. S. Venkatesh, and K. Rathnakumar, Ionics **27**, 2967 (2021). DOI: 10.1007/s11581-021-04041-w.
15. W. Zhang, D. Wu, Z. Li, and Y. Luo, Int. J. Appl. Electrom. Mech. **45**, 155 (2014). DOI: 10.3233/JAE-141825.
16. B. Dittrich, K.-A. Wartig, R. Mülhaupt, and B. Schartel, Polymers **6**, 2875 (2014). DOI: 10.3390/polym6112875.

17. J. Zhang, D. Shu, T. Zhang, H. Chen, H. Zhao, Y. Wang, Z. Sun, S. Tang, X. Fang, and X. Cao, J. All. Comp. **532**, 1 (2012). DOI: 10.1016/j.jallcom.2012.04.006.
18. L. Williams, A. R. Prasad, P. Sowmya, and A. Joseph, Mat. Chem. Phys. **242**, 122469 (2020). DOI: 10.1016/j.matchemphys.2019.122469.
19. R. M. Obodo, H. E. Nsude, C. U. Eze, B. O. Okereke, S. C. Ezugwu, I. Ahmad, M. Maaza, and F. I. Ezema, Curr. Res. Gre. Sustain. Chem. **5**, 100345 (2022). DOI: 10.1016/j.crgsc.2022.100345.
20. O. S. Ali and D. E. Al-Mammar, Iraqi J. Sci. **65**, 1824 (2024). DOI: 10.24996/ijs.2024.65.4.4.
21. S. Fatimah, R. Ragadhita, D. F. A. Husaeni, and A. B. D. Nandiyanto, ASEAN J. Sci. Eng. **2**, 12 (2021). DOI: 10.17509/ajse.v2i1.37647.
22. N. A. Khudhair and A. K. M. A. Al Sammarraie, J. Eng. Appl. Sci. **14**, 2 (2020).
23. N. A. Khudhair and A. K. M. A. Al Sammarraie, J. Glob. Pharm. Tech. **11**, 76 (2009).
24. A. S. Maged and L. S. Ahamed, Eurasian Chem. Commun. **3**, 461. DOI: 10.22034/ecc.2021.279489.1158.
25. M. A. Abdul-Zahra and N. M. Abbass, Iraqi J. Sci. **65**, 623 (2024). DOI: 10.24996/ijs.2024.65.2.4.
26. D. Andriani, S. Revianti, and W. Prananingrum, Biodiver. J. Bio. Diver. **21**, 2521 (2020). DOI: 10.13057/biodiv/d210625.
27. B. A. Hasan, Iraqi J. Phys. **16**, 32 (2018). DOI: 10.30723/ijp.v16i37.74.
28. H. Sha, W. Zheng, F. Shi, X. Wang, and W. Sun, Int. J. Electrochem. Sci. **11**, 9656 (2016). DOI: 10.20964/2016.11.21.
29. A. H. Al-Husseini, W. R. Saleh, and A. K. M. A. Al Sammarraie, J. Nano Res. **56**, 98 (2019). DOI: 10.4028/www.scientific.net/JNanoR.56.98.
30. N. P. Rumjit, P. Thomas, C. W. Lai, and Y. H. Wong, J. Electrochem. Soci. **168**, 027506 (2021). DOI: 10.1149/1945-7111/abdee7.
31. N. Van Hieu, P. Thi Hong Van, L. Tien Nhan, N. Van Duy, and N. Duc Hoa, Appl. Phys. Lett. **101**, 253106 (2012). DOI: 10.1063/1.4772488.
32. M. Beaula Ruby Kamalam, S. S. R. Inbanathan, B. Renganathan, and K. Sethuraman, Mat. Sci. Eng. B **263**, 114843 (2021). DOI: 10.1016/j.mseb.2020.114843.

حساسية المواد النانوية المحضرة حديثاً لغاز NO2 وأهميتها على السلامة البيئية والصناعية

ساره ذوالفقار جميل[1] و باسم إبراهيم العبدلي[1,2]
[1]قسم الكيمياء، كلية العلوم، جامعة بغداد، بغداد، العراق
[2]قسم البايولوجي، كلية العلوم، جامعة الاوروك

الخلاصة

برز مركب البولي أنيلين (PANI) وثاني أكسيد المنجنيز (MnO_2) المخدّر بأكسيد النيكل (NiO) كمواد واعدة لتطبيقات استشعار الغازات بسبب الموصلية العالية ومساحة السطح. تعمل هذه الدراسة على تحسين حساسية المركبات النانوية المصنعة من PANI/MnO_2:NiO تجاه غاز NO_2. تم استخدام الفحص المجهري للقوة الذرية (AFM)، والأشعة تحت الحمراء الناقلة لفوريه (FTIR)، والفحص المجهري الإلكتروني الماسح (SEM)، وتحليل الأشعة السينية المشتتة للطاقة (EDS)، وحيود الأشعة السينية (XRD) لتحليل المركبات النانوية المنتجة. تم فحص طرق أكثر دقة لتحديد المشاكل المرتبطة بالأكسدة والتآكل ونشاط المستشعر، مثل زيادة كمية أكسيد النيكل المضافة، وتغيير بنية المركبات النانوية، وتنظيم درجة حرارة العمل والرطوبة. واستنادًا إلى نتائج هذه الدراسة، من المهم فهم مدى حساسية المواد النانوية لغاز ثاني أكسيد النيتروجين لأن التعرض لهذا الملوث يمكن أن يؤثر سلبًا على البيئة وصحة الإنسان. ويمكن وضع استراتيجيات للحد من آثاره وتحسين السلامة الصناعية والبيئية بناءً على كيفية تفاعل المواد النانوية مع غاز ثاني أكسيد النيتروجين. كما ندرس أيضًا مضادات الأكسدة ومركبات النانو PANI/MnO2:NiO النانوية لخصائصها المضادة للتآكل لضمان ثبات طويل الأمد مع توصيل المستشعر. يجب إضافة مواد قوية مضادة للأكسدة ومقاومة للتآكل إلى المستشعر لإطالة عمره الافتراضي والحفاظ على أدائه في ظل ظروف التشغيل الصعبة. دمج هذه المستشعرات

الكلمات المفتاحية: بولي أنيلين، مستشعر الغاز، المتراكبات النانوية، زمن الاستجابة، زمن الاسترداد.